

Author Correction: Discovery of rapid whistlers close to Jupiter implying lightning rates similar to those on Earth

Ivana Kolmašová , Masafumi Imai , Ondřej Santolík , William S. Kurth, George B. Hospodarsky, Donald A. Gurnett, John E. P. Connerney and Scott J. Bolton

Correction to: *Nature Astronomy* <https://doi.org/10.1038/s41550-018-0442-z>, published online 6 June 2018.

In the version of this Letter originally published, in the second sentence of the last paragraph before the Methods section the word ‘altitudes’ was mistakenly used in place of the word ‘latitudes’. The sentence has now been corrected accordingly to: ‘Low-dispersion class 1 events indicate that low-density ionospheric regions predominantly occur in the northern hemisphere at latitudes between 20° and 70°’.

Published online: 20 June 2018

<https://doi.org/10.1038/s41550-018-0530-0>

Discovery of rapid whistlers close to Jupiter implying lightning rates similar to those on Earth

Ivana Kolmašová^{1,2*}, Masafumi Imai³, Ondřej Santolík^{1,2}, William S. Kurth³, George B. Hospodarsky³, Donald A. Gurnett³, John E. P. Connerney⁴ and Scott J. Bolton⁵

Electrical currents in atmospheric lightning strokes generate impulsive radio waves in a broad range of frequencies, called atmospheric whistlers. These waves can be modified by their passage through the plasma environment of a planet into the form of dispersed whistlers¹. In the Io plasma torus around Jupiter, Voyager 1 detected whistlers as several-seconds-long slowly falling tones at audible frequencies². These measurements were the first evidence of lightning at Jupiter. Subsequently, Jovian lightning was observed by optical cameras on board several spacecraft in the form of localized flashes of light³⁻⁷. Here, we show measurements by the Waves instrument⁸ on board the Juno spacecraft⁹⁻¹¹ that indicate observations of Jovian rapid whistlers: a form of dispersed atmospheric whistlers at extremely short timescales of several milliseconds to several tens of milliseconds. On the basis of these measurements, we report over 1,600 lightning detections, the largest set obtained to date. The data were acquired during close approaches to Jupiter between August 2016 and September 2017, at radial distances below 5 Jovian radii. We detected up to four lightning strokes per second, similar to rates in thunderstorms on Earth¹² and six times the peak rates from the Voyager 1 observations¹³.

The dataset we used for this analysis comes from one of the burst modes of the Waves instrument, which measures 122.88-ms-long sequences of electric and magnetic field samples with a cadence of 50 kHz. These records are usually obtained once per second, but occasionally gaps of various lengths occur. A subset of these records, which were taken at radial distances below 5 Jovian radii, was visually searched for potential lightning-generated signals. We did not detect any cases that were similar to the Voyager 1 observations of whistlers, which would have appeared as very slowly falling tones in our records. However, we found many impulsive signals with extremely rapidly falling frequencies lasting for only several milliseconds to several tens of milliseconds. These were closer to the timescales of terrestrial atmospheric whistlers than the timescales of Jovian whistlers previously detected by Voyager 1. The most relevant previously reported observations were related to dispersed atmospheric whistlers (also known as 0+ whistlers or fractional-hop whistlers), which can be detected propagating outwards from the Earth in the topside ionosphere¹⁴ but, nevertheless, still have larger durations (hundreds of milliseconds, typically) than the impulsive signals we discovered at Jupiter. These Jovian ‘rapid’ whistlers have not been observed in the past and their short duration has not been modelled in previous studies.

Examples of our observations are given in Fig. 1, which shows the results of a frequency–time analysis of the recorded magnetic field. Analysis of relative phases of the magnetic and electric field signals suggests a systematic upward propagation of Jovian rapid whistlers from the planet (see Methods and Supplementary Fig. 1), thus confirming their sources to be below the spacecraft and possibly to be lightning discharges in the Jovian atmosphere. However, if the detected electromagnetic waves propagated from the atmosphere through the ionospheric plasma medium, they would accumulate a frequency-dependent delay that would reflect the properties of the Jovian ionosphere below the spacecraft. This delay then might form the observed frequency–time shape of the Jovian rapid whistlers. A simple model based on the accumulation of the group delay along the field-aligned propagation path of right-hand polarized electromagnetic waves in a cold plasma (see Methods and Supplementary Fig. 10) yielded the results shown by dotted lines in Fig. 1. These results fit the observations surprisingly well, using realistic magnetic field and plasma density models. Thus, we conclude that the observed signals not only propagate from sources below Juno, but also that they need to traverse the ionosphere and, therefore, their origin is probably in the Jovian atmosphere.

In our selection of events for an initial systematic analysis of this new phenomenon, we only included cases with clear impulsive broadband signatures at frequencies below 10 kHz containing Jovian rapid whistlers with different rates of downward frequency drift. We excluded cases with an upward frequency drift, as well as events at frequencies above 10 kHz that might also be related to lightning (Supplementary Fig. 2) but with a different mode of propagation through the ionosphere. Our search yielded a total number of 1,627 detections of separate Jovian rapid whistlers contained in 1,311 waveform records. This number is much larger than the combined number of lightning events obtained from all previous reports^{4-7,13,15-17}.

To approximate the location of the sources, we must take into account that the electromagnetic pulse from lightning does not propagate to the spacecraft along a straight line, as it is influenced by the presence of plasma in the strong magnetic field of Jupiter. Here, we can use a simple analogy with the propagation of whistlers at Earth, where field-aligned plasma density irregularities may lead to ducted propagation along the magnetic field lines. This is assumed in Fig. 2, where our observations are projected from Juno to the bottom of the ionosphere using the Jovian surface magnetic field model (VIP4)¹⁸ and compared with previous observations. Without the assumption of ducted propagation, the expected sources would shift

¹Department of Space Physics, Institute of Atmospheric Physics, The Czech Academy of Sciences, Prague, Czechia. ²Faculty of Mathematics and Physics, Charles University, Prague, Czechia. ³Department of Physics and Astronomy, University of Iowa, Iowa City, IA, USA. ⁴NASA/Goddard Spaceflight Center, Greenbelt, MD, USA. ⁵Space Science Department, Southwest Research Institute, San Antonio, TX, USA. *e-mail: iko@ufa.cas.cz

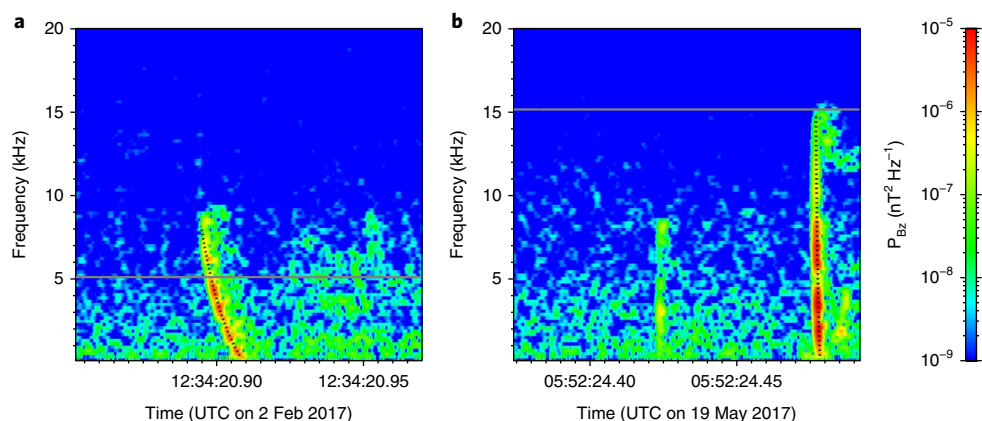


Fig. 1 | Examples of observed Jovian rapid whistlers. Frequency–time power spectrograms of the magnetic field fluctuations. **a**, Burst mode record measured on 2 February 2017 after 12:34:20 UTC at an altitude of 25,100 km above the 1 bar level. **b**, Burst mode record measured on 19 May 2017 after 05:52:24 UTC at an altitude of 7,380 km and containing two separate Jovian rapid whistlers. The horizontal grey lines show the local proton cyclotron frequency calculated from measurements of the vector magnetometer (MAG) instrument²⁷. The black dotted lines were calculated from a field-aligned propagation model of electromagnetic waves in a cold plasma, with causative discharges respectively occurring 105 and 32 ms before the arrival of the modelled Jovian rapid whistlers in **a** and **b** (see Methods and Supplementary Fig. 10). Sound files are available in the Supplementary Information.

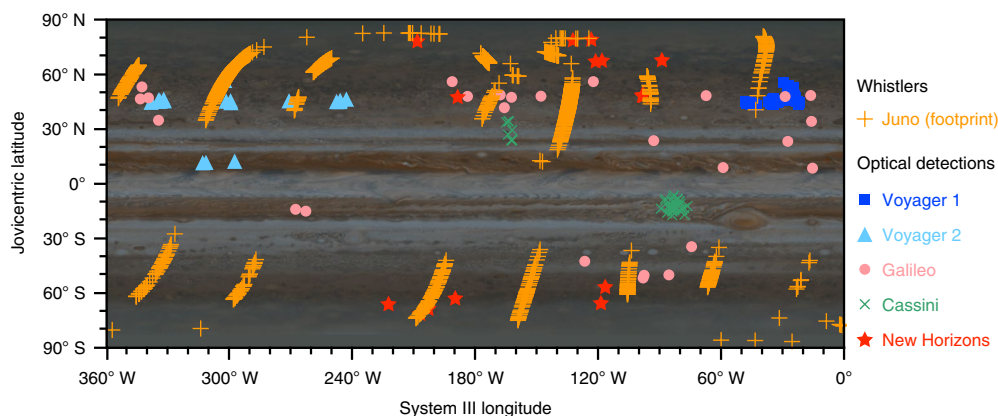


Fig. 2 | Map of lightning detections by the Juno Waves instrument compared with previous observations. Projections along the model magnetic field lines from the Juno position down to an altitude of 300 km above the 1 bar level (which we assume is the bottom of the ionosphere) are plotted for 1,627 Jovian rapid whistlers by orange ‘+’ signs, which also roughly indicate estimated uncertainties of lightning positions. Previous lightning observations are plotted for comparison: blue squares, Voyager 1 (36 lightning detections¹⁵); light blue triangles, Voyager 2 (18 detections⁴); pink dots, Galileo (estimated 336 flashes in 28 storms^{5,16}); green crosses, Cassini (approximately 50 flashes in 4 spots⁶); red stars, New Horizons (18 flashes⁷). Electromagnetic detection by the Galileo probe¹⁷, and whistler observations by Voyager 1 (167 cases¹³) near the footprints of field lines passing through the high-density Io torus are not shown. The background map was provided by NASA/JPL/Space Science Institute (<https://photojournal.jpl.nasa.gov/catalog/PIA07782>).

to lower latitudes, inducing a correction estimated to be 10–15° at low latitudes, 5–10° at mid-latitudes and below 5° at high latitudes. This correction would shift the sources towards positions defined by simple vertical projections (Supplementary Fig. 3). The main properties of the estimated source locations remain valid in any case: lightning discharges occur at mid-latitudes, although isolated cases of polar lightning are also observed. Note that the number of Jovian rapid whistlers might be underestimated at high latitudes, as most of them would be masked by intense plasma waves occurring at the same frequencies in the polar cap and auroral region^{19,20}. The lack of detections in the tropics might be a simple consequence of propagation of Jovian rapid whistlers in field-aligned ducts, which would not allow them to reach Juno’s altitude. However, the prevailing mid-latitude occurrence of Jovian lightning also seems to be indicated by initial comparison with microwave ‘sferic’ signals observed by the microwave radiometer (MWR) instrument²¹.

This global qualitative pattern can be quantified in terms of average lightning rates as a function of planetocentric latitude.

In Fig. 3 we accumulated all detected Jovian rapid whistlers in 5° intervals of footprint latitude and normalized their number by the total duration of measurement records obtained in the same latitudinal intervals at radial distances below 5 Jovian radii. The results show the largest average values (above 1 lightning stroke per second) between 40°N and 55°N magnetic latitude and only above 1 lightning stroke per 2 s between 50°S and 65°S. This difference is significant, reaching more than 3 σ estimated from Poisson statistics. However, not all individual Juno orbits show the same relationship between rates in the two hemispheres. This may also indicate a significant dependence of lightning rates on longitude (as is illustrated in Supplementary Figs. 8 and 9). Better longitudinal coverage will be obtained from upcoming Juno measurements and will allow us to separate latitudinal and longitudinal effects.

The peak latitudes move by 5–10° towards the equator for vertical projections of the source positions (black lines in Fig. 3b), which also gives us an estimate of experimental uncertainties linked to the unknown path of wave propagation. The observed average

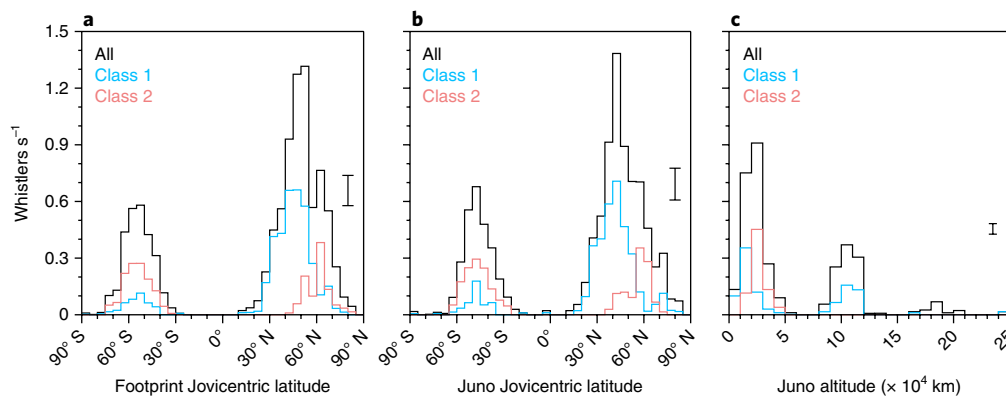


Fig. 3 | Lightning rates as a function of latitude and altitude. **a**, Average number of Jovian rapid whistlers per second in 5° wide bins of the Juno magnetic footprint latitude. **b**, The same quantity but in 5° wide bins of the vertically projected Juno latitude. **c**, The same quantity but in 10^4 km high bins of Juno altitude above the 1 bar level. The black lines show the results for all detected events. The blue lines correspond to selected events with low dispersion (class 1). The red lines correspond to selected events with higher dispersion (class 2). Error bars for the 2σ interval around the mean value of the Poisson distribution are shown on the right-hand side of each panel. They indicate that the main features of the obtained lightning rates are statistically significant.

occurrence rate is up to 10 times higher than the average rate of 0.12 whistlers s^{-1} from Voyager 1 measurements. The Voyager 1 whistlers were localized to field lines of the high-density Io torus²², which is magnetically connected to latitudes around 65° N, outside the main occurrence peak in our observations. The rates and latitudinal distribution of the Jovian rapid whistlers discovered by Juno therefore could not be predicted from the limited set of Voyager 1 observations.

The same analysis was performed as a function of Juno altitude above the 1 bar level with an interval of 10^4 km (black line in Fig. 3c). The main peak of occurrence was observed at altitudes below 5×10^4 km. A secondary peak at altitudes of $9\text{--}12 \times 10^4$ km was also observed. The gap of occurrence between the two peaks is intriguing as we would expect a smoothly decreasing trend for higher altitudes. However, a closer look shows that the secondary peak is accumulated entirely during only two Juno orbit segments and is probably linked to the altitude at which Juno crosses the range of latitudes with the highest lightning rates (see Supplementary Fig. 4).

Returning to Fig. 1, we notice larger differences of arrival times at different frequencies in Fig. 1a than in Fig. 1b. We categorized Jovian rapid whistlers in our dataset into two dispersion classes according to the difference of propagation delays at 2 and 5 kHz, whenever this was possible. Class 1 events had a difference less than 5 ms (see example in Fig. 1b); that is, their dispersion constant¹³ D was less than $\sim 0.6 s\sqrt{\text{Hz}}$. Events with larger dispersions fell into class 2 (see example in Fig. 1a). We found that 34% of the cases fell into class 1 and 26% fell into class 2. For the remaining 40%, it was impossible to reliably determine the class, mainly because the detected frequencies did not reach both 2 and 5 kHz (see example in Supplementary Fig. 7). Figure 3c shows that class 2 events were only observed below 5×10^4 km, while class 1 events also penetrated to higher altitudes. This indicates that dispersion is generated well below Juno and that occurrence peaks in altitude reflect the latitudinal effects combined with the properties of the spacecraft orbit. Figure 3 indeed shows interesting patterns in the latitudinal distribution of the two dispersion classes. The weaker mid-latitude peak in the southern hemisphere contains more class 2 events, while the northern peak mainly contains class 1 events at latitudes below 50° . A smaller fraction of class 2 events occurred at higher latitudes, with a peak occurrence coinciding approximately with the latitudes of the magnetic footprints for Voyager 1 detections of whistlers in the Io torus.

To estimate the rates at which the Jovian rapid whistlers occur in separate orbital segments, we divided them into 5-min-long time intervals, counted events in each of these intervals and then

divided the results by the accumulated duration of measurement records contained in each interval. The peak lightning rates reached between 0.7 and more than 4 events per second during different orbits (see Supplementary Fig. 5). The observed maximum rate was 6 times higher than the peak values from Voyager 1 where a maximum of about 32 whistlers were observed during a 48-s-long data frame¹³. Our new Juno observations compare well with typical rates of 1–4 fractional-hop whistlers per second detected in low Earth orbit above a thunderstorm¹². A consistency check of our dataset shows that the times of Juno detections correspond well with a Poisson random process for which the arrival time of any Jovian rapid whistler is independent of the arrival times of other events in the dataset (for details see Supplementary Fig. 6).

Obtaining surface densities of Jovian lightning rates from their measured average rates is much less straightforward as it relies mostly on uncertain assumptions. First, we need to assume a surface area over which lightning-generated electromagnetic waves penetrate into the Jovian ionosphere. Following previous estimates²², we can assume this area to be in the order of 10^6 km². In that case, our mid-latitude average rate of 1 whistler s^{-1} gives us approximately 30 flashes $\text{year}^{-1} \text{km}^{-2}$, assuming further that we receive 100% of the signals from lightning as Jovian rapid whistlers and that Jovian lightning consists of a single stroke per flash. Preliminary results of comparison with the ‘sferics’ observed by the microwave radiometer (MWR) instrument²¹ indicate the possibility of a larger penetrating area, by a factor of a few tens, giving us a flash density on the order of 1 flash $\text{year}^{-1} \text{km}^{-2}$. This is still much larger than estimates based on Galileo optical measurements⁵ (0.004 flashes $\text{year}^{-1} \text{km}^{-2}$) or combined optical and radio frequency measurements of the Galileo descent probe¹⁷ (0.07 flashes $\text{year}^{-1} \text{km}^{-2}$). Our estimates are also much larger than initial estimates of $0.0001\text{--}0.04$ flashes $\text{year}^{-1} \text{km}^{-2}$ from Voyager 1 based on optical and whistler measurements²³. The upper bound of this estimate was later increased²² by 3 orders of magnitude, assuming detection of only 10% of lightning, and further assuming ducted propagation over the whole path to the Io torus, which was discussed as questionable in a follow-up paper¹³. In any case, our estimates of Jovian flash densities are larger than most of the previous results from Jupiter and comparable to the range of terrestrial flash densities²⁴. Similar flash densities then seem to favour the hypothesis that Jovian lightning strokes also originate from water clouds^{16,25}, possibly with precipitation and convective circulation, as we see on Earth.

The observed spectral shapes of Jovian rapid whistlers provide us with a valuable source of information about the integral

properties of the Jovian ionosphere. Low-dispersion class 1 events indicate that low-density ionospheric regions predominantly occur in the northern hemisphere at latitudes between 20° and 70°. Most of the Jovian rapid whistlers are also frequency limited by cut-offs, which haven't been thoroughly discussed in this initial study. Further analysis of this growing dataset will therefore certainly yield important new discoveries not only concerning Jovian atmospheric dynamics, but also variations of plasma density and magnetic field in the Jovian ionosphere.

Methods

Analysis of propagation directions. On the Juno spacecraft, which is spin stabilized with a period of ~30 s, and with a spin axis along the spacecraft z coordinate, we measure waveform samples from mutually perpendicular electric (E_Y) and magnetic (B_Z) antennas of the Juno/Waves instrument. These signals not only carry information about the amplitudes of the two components but also about their mutual coherence and phase. If the coherence is high, the two signals do not exhibit random phase changes and they therefore probably correspond to the same source; for example, to a lightning discharge in the Jovian atmosphere. In that case, the phase of the two signals allows us to determine whether these electromagnetic waves propagate from Jupiter, as we would expect to be the case for an event generated below the spacecraft. Since we did not measure the three-dimensional vectors of fluctuating magnetic or electric fields, we were unable to directly calculate the Poynting vector from their spectral matrices²⁶. We therefore derived a simplified procedure based on some assumptions.

First, we assume that the direction of the Poynting vector of the measured waves is close to the direction of the background Jovian magnetic field or close to the direction antiparallel to it. Under this assumption, we can calculate only one component of the Poynting vector along the x axis of the spacecraft coordinates and compare its sign with the sign of the corresponding component of the locally measured background magnetic field (the B_{0X} component can be obtained from three axial measurements of the on board fluxgate magnetometer²⁷). If the signs are the same, the waves dominantly propagate along the static magnetic field B_0 ; that is, upwards from the planet in the northern hemisphere and downwards in the southern hemisphere. If the signs are opposite, the propagation direction is antiparallel to B_0 .

For upward propagation, we therefore need to obtain the same signs in the northern hemisphere and opposite signs in the southern hemisphere. The S_X component of the Poynting vector \mathbf{S} is

$$S_X = \frac{1}{\mu_0} (E_Y B_Z - E_Z B_Y) \quad (1)$$

where μ_0 is the vacuum permeability, and E_Y , E_Z , B_Y and B_Z are components of the wave electric and magnetic field. As we only measure B_Z and E_Y , we can use mutual phases between these two signals to obtain the sign of the $E_Y B_Z$ term. We therefore have to assume that the $E_Z B_Y$ term in the expression for S_X does not change its sign; that is, that it either has the same sign as $E_Y B_Z$ or that its absolute value is lower than the absolute value of $E_Y B_Z$. This assumption is always valid for the relevant plasma wave modes (for example, for the right-hand polarized R mode) if none of B_{0X} , B_Z and E_Y is negligible.

With these assumptions, the procedure is straightforward. We use a 256 point fast Fourier transform with a Hanning window, sliding by 8 samples for both B_Z and E_Y signals over the entire duration of each measurement record (6,144 samples at a 50 kHz rate) to obtain estimates of complex spectral components b_Z and e_Y for 128 frequency intervals below 25 kHz and for 737 time intervals within a measurement record. Power spectrograms of B_Z and E_Y are calculated from the squared modulus of each complex spectral component, $P_{B_Z} = b_Z b_Z^*$ and $P_{E_Y} = e_Y e_Y^*$, respectively. We also calculate normalized complex cross-spectra from the corresponding pairs of complex spectral components as

$$P_{E_Y B_Z} = \frac{e_Y b_Z^*}{\sqrt{e_Y e_Y^*} \sqrt{b_Z b_Z^*}} \quad (2)$$

on which we apply a moving average over five frequency bins. We then obtain mutual coherence as a modulus of $P_{E_Y B_Z}$,

$$C_{E_Y B_Z} = \sqrt{(\Re P_{E_Y B_Z})^2 + (\Im P_{E_Y B_Z})^2} \quad (3)$$

Mutual phase $\phi_{E_Y B_Z}$ is obtained as a complex phase of $P_{E_Y B_Z}$ after including a frequency-dependent phase calibration ϕ_C ,

$$\phi_{E_Y B_Z} = \tan^{-1} \frac{\Im P_{E_Y B_Z}}{\Re P_{E_Y B_Z}} + \phi_C \quad (4)$$

If the mutual coherence $C_{E_Y B_Z}$ is close to 1 and the magnetic field component B_{0X} is not negligible (for example, if $|B_{0X}|$ is larger than 1% of the total field strength $|B_0|$), the mutual phase $\phi_{E_Y B_Z}$ indicates whether the wave is propagating upwards or downwards. In the northern hemisphere, a combination of positive B_{0X} with $\phi_{E_Y B_Z}$ close to 0° indicates upgoing waves while for negative B_{0X} we need to have $\phi_{E_Y B_Z}$ close to 180° for upgoing waves. This is opposite in the southern hemisphere. Supplementary Figs. 1 and 2 show examples of upgoing waves in the northern hemisphere for positive and negative B_{0X} , respectively.

During the preparation of our dataset of Jovian rapid whistlers, we found only 16 detections for which the phase indicated propagation towards the planet, and 4 detections where the phase gave unclear results, with $\phi_{E_Y B_Z}$ being around -45° or -90°. To be conservative, all these cases were removed from our dataset, which then contained a total of 1,627 events, of which 1,422 had a phase indicating outward propagation from Jupiter. For the remaining 205 events, we either detected only one of the signals or B_{0X} was negligible and we were therefore unable to determine the phase $\phi_{E_Y B_Z}$. We kept this group in the dataset as, taking into account the above results, it was very probable that we would also obtain upward propagation for these cases.

A simple model of propagation delays. Assuming a simple model of electromagnetic waves propagating along the magnetic field lines in a cold electron-proton plasma, we can verify the consistency of the measured frequency drift with the expected profile of the plasma density and the Jovian magnetic field strength. The procedure consists of accumulating propagation delays at each frequency along the propagation path by numerical evaluation of an integral

$$t - t_0 = \int_0^L v_G^{-1} dl \quad (5)$$

where t_0 is the time of the passage of the lightning-generated electromagnetic pulse through the 1 bar level, L is the length of the magnetic field line from the 1 bar level up to the spacecraft and v_G is the group velocity obtained from the cold plasma theory²⁸. From the possible cold plasma wave modes, we select a solution giving the same sense of rotation of the electric field vector as the sense of cyclotron motion of electrons; that is, the right-hand polarized R mode. The group velocity at each point along the propagation path depends on the wave frequency, local magnetic field strength and local plasma density.

For our calculations, we obtain the profile of the magnetic field strength $B_0(\mathbf{r})$ from the Jovian VIP4²⁸ model by its recalibration to the measured field strength $B_0(\mathbf{r}_p)$ at the Juno position \mathbf{r}_p ,

$$B_0(\mathbf{r}) = M B_{0M}(\mathbf{r}), M = \frac{B_0(\mathbf{r}_p)}{B_{0M}(\mathbf{r}_p)} \quad (6)$$

where $B_{0M}(\mathbf{r})$ is obtained from the VIP4 model. Values of the multiplicative calibration coefficient M vary from case to case. For example, $M = 1.08$ for Fig. 1a and $M = 1.21$ for Fig. 1b.

The plasma density profile is taken from the Voyager 2 entry radio occultation measurements²⁹, which were obtained for the afternoon local time of 17.7 h, similar to local times of 16.1 and 17.0 h of the measurements from Fig. 1a and b, respectively. The latitude of the Voyager 2 measurements (66°S) is in absolute value close to the latitude of the magnetic footprint for the case from Fig. 1a (64.5°N) but differs from the magnetic footprint latitude of the case from Fig. 1b (33.5°N). Supplementary Fig. 10 demonstrates that this radio occultation density profile shows a sharp peak of $3.5 \times 10^5 \text{ cm}^{-3}$ at an altitude of 640 km above the 1 bar level and an exponential decrease at altitudes above 1,500 km. As the upper limit of this model is 4,000 km in altitude, we used a least-squares fit of an exponential model,

$$n = n_0 \exp\left(-\frac{h}{H}\right) \quad (7)$$

for experimental points at altitudes h above 1,640 km, yielding $n_0 = 1.43 \times 10^5 \text{ cm}^{-3}$ and the characteristic scale height of the topside ionospheric density decrease $H = 968 \text{ km}$. We use this numerical exponential extension of the Voyager 2 entry radio occultation model²⁹ for altitudes above 1,640 km (see Supplementary Fig. 10).

The observed event from Fig. 1a agrees with model calculations according to equation (5) using the above described magnetic field and plasma density models (see Supplementary Fig. 10). For the event from Fig. 1b, the recalibrated magnetic field model from equation (6) gives a field almost twice as strong as for the case in Fig. 1a. This is linked to longitudinal variations of the magnetic field strength, as is demonstrated in Supplementary Fig. 9. For example, at the altitude of the peak of the ionospheric plasma density at 640 km, we obtain a magnetic field strength of 1,515 μT for the case in Fig. 1b compared with a field strength of 815 μT for the case in Fig. 1a. This larger magnetic field strength causes smaller differences in the group velocity profiles at different frequencies and hence a slightly lower dispersion of the modelled event. However, the observed case from Fig. 1b still has much lower dispersion than this model.

The model starts to correspond to the observations in Fig. 1b only when we artificially decrease all the density values to 10% of the above described exponentially extended Voyager 2 entry radio occultation model (see Supplementary Fig. 10). This modified profile gives a peak density of $3.5 \times 10^4 \text{ cm}^{-3}$, which is still roughly comparable to the Galileo radio occultation profiles³⁰. This is also a relatively reliable result, as decreasing the densities to 20% gives a larger dispersion that visibly does not fit the observations (not shown). Another hypothetical possibility for obtaining agreement with the measured dispersion in Fig. 1b would be to increase the magnetic field strength by a factor of 2 in the region of the ionospheric peak while keeping the same density model as for Fig. 1a.

This simple model does not explain the observed upper-frequency cutoffs of Jovian rapid whistlers. However, if we allow the wave vectors to deviate from the tangent direction to the local field line, we obtain sudden decreases in the group velocity at the characteristic frequencies of the plasma medium. As slight deviations from the exactly field-aligned propagation can be expected even in the density ducts, the upper cutoff in Fig. 1b can be explained by the local proton cyclotron frequency. In the case of Fig. 1a the cutoff might be caused by the local plasma frequency. It would then be higher than predictions from the exponential model (equation (7)), but without significant effects on accumulated dispersion (equation (5)) if the ionospheric densities remained the same. However, the accumulated dispersion might be significantly influenced by propagation at higher wave vector angles with respect to the magnetic field lines, which would change the frequency-dependent group velocity in equation (5). Analysis of these possible effects requires a more complex ray-tracing calculation, which will be the subject of a future study.

Data availability. The data used in this paper are available at the Planetary Data System: <https://pds.nasa.gov/>. The data that support the plots within this paper and other findings of this study are available from the corresponding author upon reasonable request. The list of previous observations of lightning is available as Supplementary Data 1. The list of measurement intervals with whistlers is available as Supplementary Data 2. The data format of both datasets is described in Supplementary Tables 1 and 2, respectively.

Received: 31 January 2018; Accepted: 7 March 2018;
Published online: 6 June 2018

References

- Storey, L. R. O. An investigation of whistling atmospherics. *Phil. Trans. R. Soc. Lond. A* **246**, 113–141 (1953).
- Gurnett, D. A., Shaw, R. R., Anderson, R. R., Kurth, W. S. & Scarf, F. L. Whistlers observed by Voyager 1: detection of lightning on Jupiter. *Geophys. Res. Lett.* **6**, 511–514 (1979).
- Smith, B. A. et al. The Jupiter system through the eyes of Voyager 1. *Science* **204**, 951–957 (1979).
- Borucki, W. J. & Magalhaes, J. A. Analysis of Voyager 2 images of Jovian lightning. *Icarus* **96**, 1–14 (1992).
- Little, B. et al. Galileo images of lightning on Jupiter. *Icarus* **142**, 306–323 (1999).
- Dyudina, U. A. et al. Lightning on Jupiter observed in the H α line by the Cassini imaging science subsystem. *Icarus* **172**, 24–36 (2004).
- Baines, K. H. et al. Polar lightning and decadal-scale cloud variability on Jupiter. *Science* **318**, 226–229 (2007).
- Kurth, W. S. The Juno Waves Investigation. *Space Sci. Rev.* **213**, 347–392 (2017).
- Bolton, S. J., Levin, S. M. & Bagenal, F. Juno's first glimpse of Jupiter's complexity. *Geophys. Res. Lett.* **44**, 7663–7667 (2017).
- Bolton, S. J. et al. Jupiter's interior and deep atmosphere: the initial pole-to-pole passes with the Juno spacecraft. *Science* **356**, 821–825 (2017).
- Connerney, J. E. P. et al. Jupiter's magnetosphere and aurorae observed by the Juno spacecraft during its first polar orbits. *Science* **356**, 826–832 (2017).
- Fiser, J., Chum, J., Diendorfer, G., Parrot, M. & Santolík, O. Whistler intensities above thunderstorms. *Ann. Geophys.* **28**, 37–46 (2010).
- Kurth, W. S., Strayer, B. D., Gurnett, D. A. & Scarf, F. L. A summary of whistlers observed by Voyager 1 at Jupiter. *Icarus* **61**, 497–507 (1985).
- Santolík, O., Parrot, M. & Chum, J. Propagation spectrograms of whistler-mode radiation from lightning. *IEEE Trans. Plasma Sci.* **36**, 1166–1167 (2008).
- Williams, M. A. *An Analysis of Voyager Images of Jovian Lightning* (Univ. Arizona, University Microfilms International, Ann Arbor, 1986).
- Gierasch, P. et al. Observation of moist convection in Jupiter's atmosphere. *Nature* **403**, 628–30 (2000).
- Rinnert, K. et al. Measurements of radio frequency signals from lightning in Jupiter's atmosphere. *J. Geophys. Res. Planets* **103**, 22979–22992 (1998).
- Connerney, J. E. P., Acuña, M. H., Ness, N. F. & Satoh, T. New models of Jupiter's magnetic field constrained by the Io flux tube footprint. *J. Geophys. Res. Space Phys.* **103**, 11929–11939 (1998).
- Tetrick, S. S. et al. Plasma waves in Jupiter's high-latitude regions: observations from the Juno spacecraft. *Geophys. Res. Lett.* **44**, 4447–4454 (2017).
- Kurth, W. S. et al. A new view of Jupiter's auroral radio spectrum. *Geophys. Res. Lett.* **44**, 7114–7121 (2017).
- Brown, S. et al. Prevalent lightning sferics at 600 megahertz near Jupiter's poles. *Nature* <https://doi.org/10.1038/s41586-018-0156-5> (2018).
- Scarf, F. L., Gurnett, D. A., Kurth, W. S., Anderson, R. R. & Shaw, R. R. An upper bound to the lightning flash rate in Jupiter's atmosphere. *Science* **213**, 684–685 (1981).
- Lewis, J. S. Lightning on Jupiter: rate, energetics, and effects. *Science* **210**, 1351–1352 (1980).
- Christian, H. J. Global frequency and distribution of lightning as observed from space by the Optical Transient Detector. *J. Geophys. Res.* **108**, 4005 (2003).
- Ingersoll, A., Gierasch, P., Banfield, D. & Vasavada, A. Moist convection as an energy source for the large-scale motions in Jupiter's atmosphere. *Nature* **403**, 630–632 (2000).
- Santolík, O. et al. Survey of Poynting flux of whistler mode chorus in the outer zone. *J. Geophys. Res.* **115**, 1–13 (2010).
- Connerney, J. E. P. et al. The Juno Magnetic Field Investigation. *Space Sci. Rev.* **213**, 39–138 (2017).
- Gurnett, D. A. & Bhattacharjee, A. *Introduction to Plasma Physics With Space, Laboratory and Astrophysical Applications* 2nd edn (Cambridge Univ. Press, Cambridge, 2017).
- Hinson, D. P., Twicken, J. D. & Karayel, E. T. Jupiter's ionosphere: new results from Voyager 2 radio occultation measurements. *J. Geophys. Res. Space Phys.* **103**, 9505–9520 (1998).
- Hinson, D. P. et al. Jupiter's ionosphere: results from the First Galileo Radio Occultation Experiment. *Geophys. Res. Lett.* **24**, 2107 (1997).

Acknowledgements

We acknowledge all members of the Juno mission team, especially the engineers and staff of the Juno Waves instrument. The research at the University of Iowa was supported by NASA through contract 699041X with the Southwest Research Institute. The work of I.K. and O.S. was supported by the MSM100421701 and LTAUSA17070 grants and the Praemium Academiae award.

Author contributions

I.K. and M.I. independently performed extensive searches for Jovian rapid whistlers in the Waves burst dataset and combined the results in common list of events. M.I. and O.S. prepared the occurrence maps and calculated occurrence rates from this list. W.S.K., G.B.H. and D.A.G. provided consultations on data analysis. W.S.K. is responsible for the Juno Waves instrument. J.E.P.C. provided the planetary magnetic field measurements. S.J.B. is principal investigator of the Juno spacecraft. The manuscript was written by O.S. and I.K. with input from all authors.

Competing interests

The authors declare no competing interests.

Additional information

Supplementary information is available for this paper at <https://doi.org/10.1038/s41550-018-0442-z>.

Reprints and permissions information is available at www.nature.com/reprints.

Correspondence and requests for materials should be addressed to I.K.

Publisher's note: Springer Nature remains neutral with regard to jurisdictional claims in published maps and institutional affiliations.

Author Correction: Discovery of rapid whistlers close to Jupiter implying lightning rates similar to those on Earth

Ivana Kolmašová , Masafumi Imai , Ondřej Santolík , William S. Kurth, George B. Hospodarsky, Donald A. Gurnett, John E. P. Connerney and Scott J. Bolton

Correction to: *Nature Astronomy* <https://doi.org/10.1038/s41550-018-0442-z>, published online 6 June 2018.

In the version of this Letter originally published, in the second sentence of the last paragraph before the Methods section the word ‘altitudes’ was mistakenly used in place of the word ‘latitudes’. The sentence has now been corrected accordingly to: ‘Low-dispersion class 1 events indicate that low-density ionospheric regions predominantly occur in the northern hemisphere at latitudes between 20° and 70°’.

Published online: 20 June 2018

<https://doi.org/10.1038/s41550-018-0530-0>